THEORETICAL AND EXPERIMENTAL STUDIES OF THE SPATIAL SENSITIVITY OF AN ELECTROSTATIC PULVERISED FUEL METER

Dr. Jianyong Zhang, Emeritus Professor John Coulthard
School of Science and Technology, University of Teesside, Middlesbrough, UK

Abstract:
In coal-fired power plants, the coal is pulverised and pneumatically conveyed to the burners. It is essential to measure and control pulverised fuel (PF) to improve combustion efficiency; reduce pollution and lower operating costs. Unlike single-phase flow, where flow density is generally considered to be uniform, air-solids two-phase flow in pneumatic conveying systems can undergo inhomogeneous concentration distributions across a given pipe cross-sectional area, especially around bends and bifurcators or trifurcators. The "roping" flow regime is an extreme example of inhomogeneous solids distribution, where highly concentrated solids form a column-like (rope-like) flow.
For such complex flow regimes, solids concentration or solids mass flow meters will give different outputs when inhomogeneous flow occurs at locations where these meters are installed if they are sensitive to the flow patterns. This problem can be solved in two ways. The first and simplest approach is to restrict the meter's installation to locations where solids are relatively uniformly distributed over the cross-sectional area of the pipe. Alternatively, it can be solved by using a meter having uniform spatial sensitivity, so that the measurement would not be affected by the flow regimes.
Because the installation locations of PF meters must suit other requirements, such as accessibility for the convenience of maintenance, it is ideal if the meters have uniform spatial sensitivities.
Electrostatic mass-flow meters are typically used to give a measure of the fuel mass flow rate. One design employs ring-shaped electrodes which have non-uniform sensitivity, resulting in variations in meter output for the same flow stream passing through the sensing volume at the different radii relative to the meter's central line. This paper presents a theoretical analysis of the spatial sensitivity of the electrostatic meter with

ring-shaped electrodes in the time and frequency domains. One goal of the study is to improve its performance and to achieve uniform sensitivity.

The experimental data presented in this paper support the overall mathematic modeling, based on electrostatic field theory, using the finite element method (FEM). Although the FEM analysis provides useful results, a more rigorous investigation is recommended for future work.

Keywords: Electrostatic pulverised fuel meter, spatial sensitivity.

Introduction

In coal-fired power plants, the fuel is pulverised, mixed with air, and pneumatically conveyed to the furnace burners. Upon leaving the pulverising mill, the mixture of solids and air is split into several different pipes, each feeding an individual burner. The typical mill can feed up to eight separate burners. Usually, the fuel and air are metered prior to their entry into the mill, so that their ratio can be set accurately. Differences in routing of the conveyors injecting the pulverised fuel (PF) into the furnace, as well as unequal distribution at the points where the incoming stream is split into separate pathways, can cause an uneven feed of pulverized coal to the burners. Consequently, the combustion stoichiometry at the burners is disturbed, resulting in localized, fuel-rich regions where there is insufficient air to burn the coal and ash with a high-carbon content. Conversely, fuel-lean regions will also occur, causing high NOx levels to appear. It is therefore desirable to measure and control the flow rate of pulverised coal supplied to each burner so as to optimise combustion.

The typical 500-MW boiler might have forty to sixty 500mm diameter burners. The volume concentration of solids, i.e. the ratio of solids volume to the volume of the mixture of air and solids fed to these burners, is very low (typically about 0.1%), hence the meters must have high sensitivity. At a conveyance velocity of about 25 m/s, the mixture becomes highly abrasive, so that no restriction to the flow can be tolerated. The PF meter described in this paper is comprised of a short steel pipe section into which ring-shaped electrodes are fitted flush with, and insulated from, the conducting pipe wall, thereby offering no restriction to the flow. Signals generated in these electrodes due to

the flowing charged particles are used to provide a measure of the solids concentration and the solids velocity, so that the mass-flow rate of the fuel to each burner can be inferred from these two parameters.

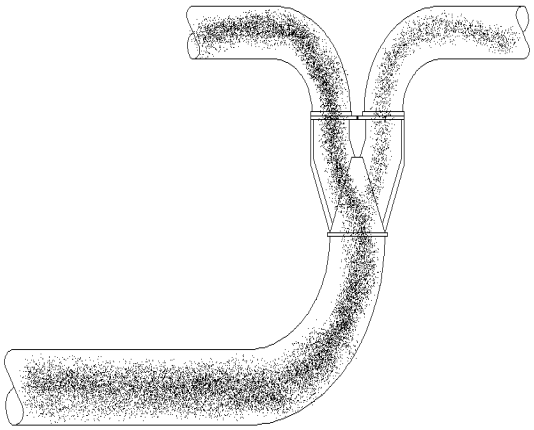

Fig.1 An Example of "roping" Flow around a Bifurcator

The distribution of solids over the cross section of a pneumatic conveying pipe has been investigated by Huber, [1], Bernard J Barry et al [2], Yilmaz et al [3], and Frank [4]. From their studies, it was concluded that the solids can undergo inhomogeneous concentration distributions across a given pipe cross-sectional area. Such distributions are affected by the conveyance velocity, particle size, humidity, and conveyor geometry. The so-called "roping" flow regime is an extreme example of inhomogeneous distribution where inside the "rope", the highly concentrated solids flow is formed, as illustrated in Fig. 1.

Ideally, if the meter is designed to measure the solids mass flow rate, it should have the same output in response to the solids stream carrying identical solids mass flow wherever it passes through within the meter's sensing volume. In other words, the meter should have a uniform spatial sensitivity which is defined in this paper as the ratio of the root-mean-square value of the signal produced by the meter to the mass flow rate of a "roping flow" in parallel with the pipe centre line measured at different axial positions at a given flow velocity. However, the charges induced in the electrodes and the rms value of the output of the meter depend on the solids stream position relative to the pipe centre line.

Although the passive electrostatic pulverised-fuel meter has a number of advantages over other meters, it does not have a uniform spatial sensitivity as do similar techniques such as the capacitive pulverised fuel meter [5] or electrostatic probe [6] and probes based on laser systems [7]. Improving of the performance of the PF meter involves several issues, some of which are still the subject of ongoing investigations [8-11]. One primary issue is

directed to achieving uniform spatial sensitivity hence it is necessary to study the spatial sensing characteristics of this type of meter to achieve that goal.

Velocity measurement

The velocity of the flowing solids is measured using two ring-shaped electrodes placed a known distance apart. These electrodes detect variations in induced charge signals. The latter are cross-correlated to measure the flow transit time between the two electrodes.

Suppose that $x(t)$ and $y(t)$ are the signals from the upstream and downstream electrodes, respectively. The cross correlation of these signals $R_{xy}(\tau)$is given by;

$$R_{xy}(\tau) = \lim_{T\to\infty} \frac{1}{T} \int_0^T x(t-\tau)y(t)dt \qquad (1)$$

The cross correlation function is characterised by a peak occurring at a time delay τ_m that describes the transit time of the solid particles between the two electrodes. If the electrode spacing is L, then the solids velocity V is given by

$$V=L/\tau_m \qquad (2)$$

The measurement of particle velocity V in Eq. (2) is absolute, having dimensions of distance divided by time.

Solids concentration measurement

In pneumatic conveying, electrical charging of the conveyed solids occurs. The primary sources of electrification are frictional contact charging between particles, charge transfer from one particle to another, and friction between particles and the conducting pipe wall.

The fluctuation level in the net charges carried by solids is proportional to the solids concentration under the lean-phase condition. The electrostatic pulverised fuel meter described in this paper was designed to measure this fluctuation to indicate solids concentration and solids mass flow rate. These can be calculated if the solids velocity is known.

Figure 2 shows a simplified, schematic view of the signal-detecting system studied in this paper. The ring-shaped metallic electrode is installed flush with the inner surface of the

earthed conveyor. The electrode is insulated from the conducting conveyor wall but exposed to the flowing air-solid mixture and is ac coupled to an amplifier.

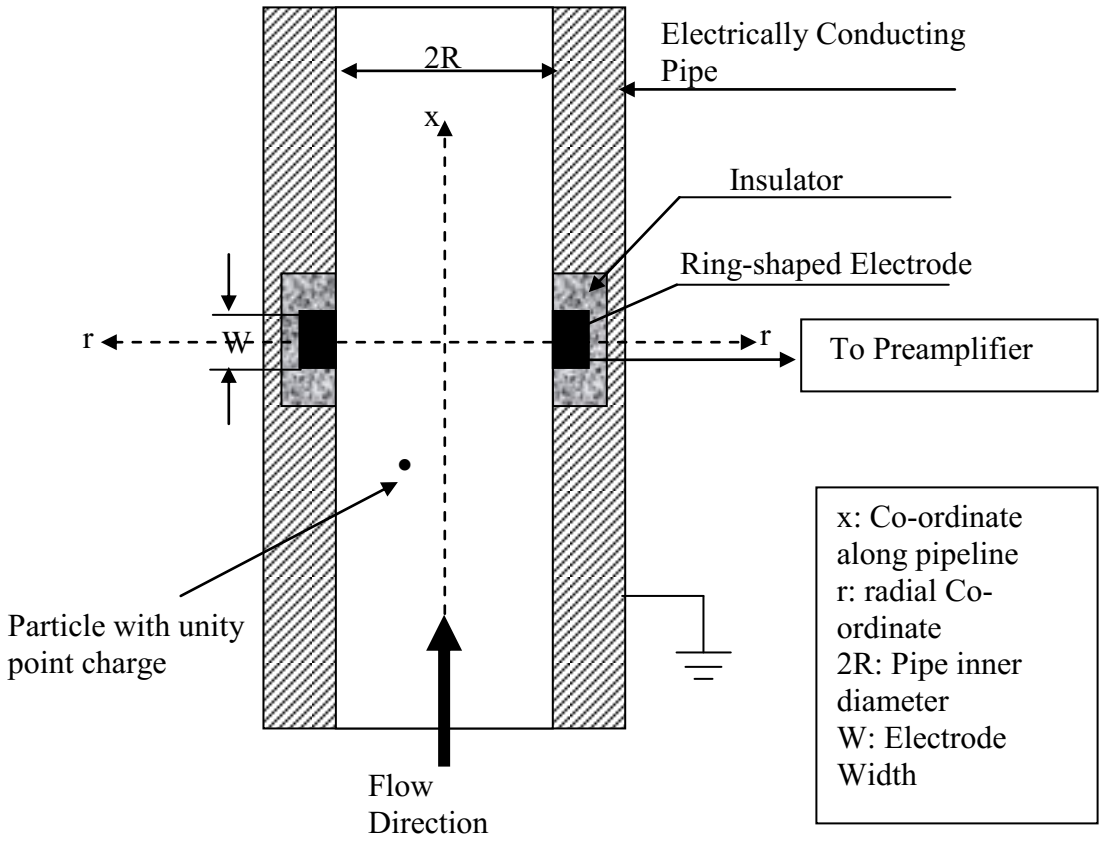

Fig. 2 Schematic of a Ring Shaped Electrode Fitted into Pneumatic Conveyor

This arrangement ensures that the electrode does not restrict the flow and is sensitive to the charges carried by the fuel particles. It also minimises the electrode wear that can occur with intrusive probes [6]. The charges are induced on the electrode when charged particles pass within its vicinity. The root mean square (rms) value of the random variations in the charges induced on the electrode is proportional to the variation in the net charges carried by flowing particles and is used as the indication of the solids concentration. It is obvious that this is not an absolute measurement of solids concentration, because the charge variation in the electrode is dependent on many properties, such as moisture content and the chemical composition of the solids. If the meter is calibrated under a given set of conditions (for example, humidity, chemical

composition of the solids, particle size distribution, etc.), the measured value cannot give true mass flow rate or concentration when the conditions change. The indication becomes only a relative measurement under conditions which are different from that of the calibration.

For control and fuel-balancing purposes, it is sufficient to measure the ratio of solids mass flow rate in each conveyor to the total mass flow rate emanating from the mill. This ratio is known as "split". Provided that the mass flow rate measured by the meter is proportional to the true mass flow rate of the fuel flowing simultaneously through each conveyor, the true split can be calculated by using the relative mass flow rate in each conveyor. Because the flow measured in each conveyor is fed from a single mill processing the same fuel, and because flow passes through each conveyor by successive division to the burners, we can expect the solids in each conveyor to have similar properties. The absolute or true solids mass-flow rate to each burner need not necessarily be known.

Example: Split measurement system

Figure 3 provides an example showing a trifurcating junction, through which solids from the mill pass through and are split into three pneumatic conveyors to which three pulverised fuel meters are fitted.

The split can be inferred from the ratio of measured solids mass flow rate on the corresponding meters.

The pulverised fuel measurement system uses one computer to acquire and process all signals derived from the electrodes and to display instantaneous values of pulverised fuel velocity, relative solids concentration, relative solids mass flow rate, and solids split for each conveyor.

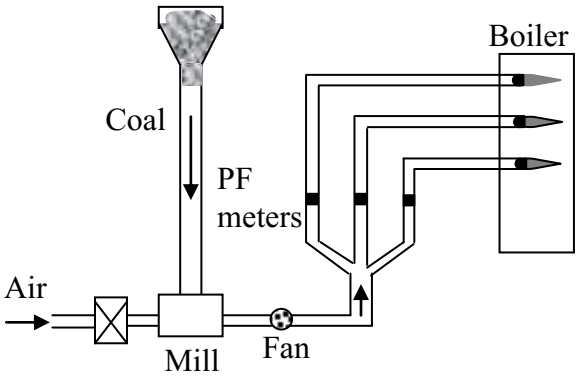

Fig. 3 An Example of Fuel Distribution

The spatial response of a ring-shaped electrode

The charge induced on a ring-shaped electrode from a single particle having unity charge has been modeled mathematically by Gajewski [12] and Cheng [13]. Cheng's model was based on electrostatic theory and calculated using the finite element method (FEM). The FEM technique is a very powerful tool for obtaining the numerical solution of a wide range of engineering problems such as stress, strain, temperature distribution, flow velocity or electric field strength [14].

As shown in Fig. 2, the charge Q induced on the inner surface of the electrode due to a particle of unity point charge inside the pipe was calculated using following expression;

$$Q = \int_S \sigma \cdot ds \tag{3}$$

Here σ is the surface density of the charge induced on the electrode, and S is entire inner surface area of the electrode.

From electrostatic theory, one can show that the charge density on the surface of a conductor is equal to the electrical flux density D.

$$\sigma = D \tag{4}$$

The following expressions also apply in the analysis,

$$\nabla \cdot D = p \tag{5}$$

$$\nabla \cdot D = \nabla \cdot \varepsilon E \tag{6}$$

$$E = -\nabla \Phi \tag{7}$$

Where p is the volume space charge, here referred to as the "source charge", E is the electric field strength, ε refers to the relative permittivity of the medium, ∇ is the gradient operator, and Φ is the electrical potential. Combining the above equations gives

$$\nabla \cdot (\varepsilon \nabla \Phi) = -p \tag{8}$$

The following boundary conditions of potential Φ on each part of the boundary of the region considered were assumed;

$$\Phi(\Gamma_p) = 0 \cup \Phi(\Gamma_i) = 0 \cup \Phi(\Gamma_t) = 0 \tag{9}$$

where Γ_p, Γ_i, Γ_t are the boundaries of the pipe, the insulator, and the electrode respectively. The insulator's potential was assumed to be zero, but it may not have been so. However, using other low potentials (2 Volts or 3 Volts) for the insulator with the finite element method produced similar results for the electric field within the sensor seems, hence the assumption seems justified. The equivalent resistance and capacitance of the electrode were not taken into account in this model. They will be considered together with the preamplifier.

The FEM analysis results were curve fitted to the following equation.

$$Q=Ae^{-k^2x^2} \qquad (10)$$

where A and k are two constants that are functions of the width W of the electrode and the radius r from the centre line of the electrode towards the pipe wall. The variable x denotes the distance along the pipeline from the centre of the electrode cross section as illustrated in Figs. 2 and 4. The quantity Q is the charge induced from a particle carrying unity point charge.

The response of the ring-shaped electrode to 'roping' flow

When pulverised flow, rather than a single point charge, is considered, the particle size and surface area must be taken into account. In addition, bipolar charging of the particles is possible. The induced signal in this case will be due to the net charge on the particles. Therefore, some assumptions must be made to permit a theoretical analysis that can be compared with experimental results.

The particles are assumed to be spherical and to have uniform particle diameter D_p , and each particle is assumed to have the same surface charge density σ_p. It is also assumed that the particles are evenly distributed within a given incremental volume, i.e. the number of solids particles within a unit volume can be described by a single variable N. The charges carried by the particles are therefore assumed to have the same polarity and value. This assumption ignores the difference between the net charge and the total negative or positive charges. In the discussions to follow, the input to the electrode is defined as the net charge carried by solids, and the output of the electrode is the charge induced on the electrode.

The ring-shaped electrode has axial symmetry; hence, for any "roping" flow that occurs in parallel with the pipeline over the electrode sensing volume, there will always be a ring-shaped

.

flow stream which produces the same charge on the electrode. In terms of the charge

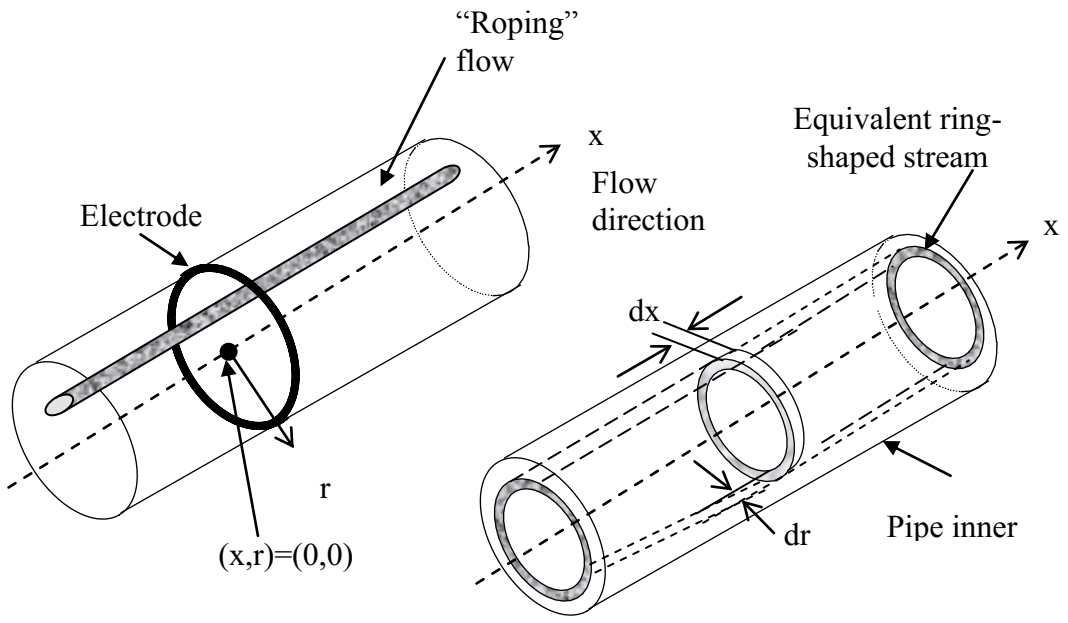

A: Hypothetic Roping flow in parallel with pipeline

B: Equivalent ring-shaped flow

Fig. 4 A "roping" Flow and Its Ring-Shaped Equivalent Stream

induced on the electrode, this ring-shaped stream is therefore the equivalent of column-shaped (roping) flow.

Figure. 4B shows a ring-shaped stream having inner radius r and outer radius $r + \Delta r$ which is the equivalent of the "roping" flow shown in Fig.4A.

In this case, A and k are functions of the electrode width W and the radial position r of the charged particles. They thus are expressed in the following equations as $A(r,W)$ and $k(r,W)$.

Based on the principle of superposition of electrostatic fields and Eq. 10, the induced charge Q_{mic} due to a hypothetical ring $\Delta r^*\Delta x$ of a micro volume within the sensing volume, shown at position (r,x) in Fig. 4, can be expressed as follows.

$$Q_{mic}=\sigma_p \cdot \pi \cdot D_p^2 N \cdot 2\pi r \cdot A(r,W)e^{-k(r,W)x^2} \Delta r \cdot \Delta x \qquad (11)$$

Let Δr approach zero, extend Δx towards the sensing length of the electrode, and divide both sides of Eq. 11 by $2\pi r^*\Delta r$ so as to guarantee that the ring contains the same amount of charge wherever the roping stream appears. The response of the electrode to the net charge carried by this hypothetical ring thus represents the spatial response at the radius r. The latter can be expressed as follows:

$$Q_{NET}^r = \sigma_p \cdot \pi \cdot D_P^2 \cdot N \int_{L_x} A(r,W)e^{-k(r,W)x^2} dx \qquad (12)$$

Here L_x is the dimension of the electrode sensing volume along the pipeline, and Q_{NET}^r *is* the charge induced on the electrode due to the net charge in this ring-shaped particle-air-mixture stream with distance r relative to the central pipe axis.

This roping particle stream can be regarded as a traveling wave of velocity V originating from the outlet of a conveyor splitting junction. In order to study the response of the electrode to a unit impulse of net charge, it is assumed that the charge carried by the solid particles is as follows:

$$Q_{NETr}^P = \sigma_p \cdot \pi \cdot D_P^2 \cdot N(t) = \delta(t-\frac{x}{V}) \qquad (13)$$

Here Q_{NETr}^P is the net charge carried by the particles of a unit impulse waveform traveling along the pipeline at radial distance r relative to the centre line of the pipe. Because time variations must be considered, the

particle number density N is re-expressed here as the time varying $N(t)$ in the above equation. It is clear that at any given time, only one point along the x direction exists where Q_{NETr}^P , or $N(t)$ is not equal to zero. This point is equal to V_t. Hence Eq. 12 becomes

$$Q_{NET}^{r} = h_{rd}(t) = A(r,W)e^{-k(r,W)V^2t^2} \qquad (14)$$

This equation describes the dynamic spatial response of a ring-shaped electrode to a ring-shaped unit impulse of net charge carried by solid particles. The variable h_{rd}(t) also represents the impulse response of the ring-shaped electrode to the mass flow rate of the solids, since it was assumed that the solids concentration is proportional to the net charge carried by solids at a given velocity.

Spatial frequency response of an electrode

Applying Fourier transformation to Eq. 14, the spatial frequency-response characteristic of a ring-shaped electrode to a unit impulse of net charge carried by particles is as follows

$$H_r(\varpi) = \int_{-\infty}^{\infty} h_{rd}(t)e^{-j\varpi t}dt = \int_{-\infty}^{\infty} A(r,W)e^{-k(r,W)V^2t^2}e^{-j\varpi t}dt = \frac{A(r,W)\pi^{\frac{1}{2}}}{V\sqrt{k(r,W)}}e^{-\frac{\varpi^2}{4V^2}\frac{1}{k(r,W)}} \qquad (15)$$

Spatial frequency response of a ring-shaped electrostatic pulverised fuel meter

In practice, the electrode must be connected to measuring equipment or to a preamplifier. An ac-coupled (differential) circuit is usually designed to detect the root mean square (*rms*) value of the ac signal components on the electrode, corresponding to the fluctuation in the net charge carried by particles. In this paper, the combination of the electrode and the electronics comprise the PF meter.

A simplified representation of an ac-coupled circuit is shown in Fig. 5. Here Q represents the charge induced on the electrode; the equivalent resistance R_n and capacitance C_n of the electrode to the earthed conveying pipe are also considered. The input resistance and capacitance

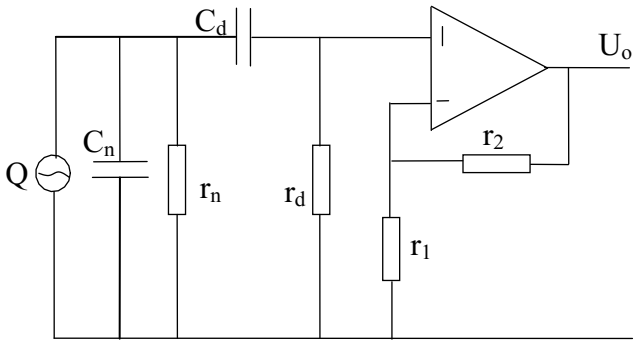

Fig. 5 ac-Coupled Voltage Amplifier

of the pre-amplifier are ignored.

A general transfer function of ac-coupled preamplifier is as follows,

$$\frac{U_o(\varpi)}{Q(\varpi)} = P(\varpi) = \frac{-\varpi^2 C_d r_d r_n (r_1 + r_2)}{(1 + j\varpi(C_n r_n + C_d r_d + C_d r_n) - \varpi^2 C_d r_d C_n r_n) r_1} \tag{16}$$

Taking the net charge carried by the solids as the input and U_o as the output of the pulverised fuel meter, the transfer function $T(\varpi)$ of the meter is the product of both the electrode and the preamplifier transfer functions. The meter's frequency spatial sensitivity therefore can be expressed as $T_r(\varpi) = H_r(\varpi)*P(\varpi)$, i.e.,

$$T_r(\varpi) = \frac{U_o(\varpi)}{Q^P_{NETr}(\varpi)} = \frac{A(r,W)\pi^{\frac{1}{2}}}{V\sqrt{k(r,W)}} e^{-\frac{\varpi^2}{4V^2}\frac{1}{k(r,W)}} * \frac{-\varpi^2 C_d r_d r_n (r_1 + r_2)}{(1 + j\varpi(C_n r_n + C_d r_d + C_d r_n) - \varpi^2 C_d r_d C_n r_n) r_1} \tag{17}$$

The values of R_n and C_n of a given electrode depend on its geometry and the insulation between the pipe wall and the electrode. Assuming that the electronics are designed to detect charge variations on the electrode that correspond only to fluctuations in the net particle charge, the power spectral function of the meter output is as follows

$$\left|U_o(\varpi)\right|^2 = \left|T_r(\varpi)\right|^2 * \left|Q^P_{NETr}(\varpi)\right|^2 \tag{18}$$

$$\left|U_o(\varpi)\right|^2 = \left|T_r(\varpi)\right|^2 * \left|q^P_{NETr}(\varpi)\right|^2 \tag{19}$$

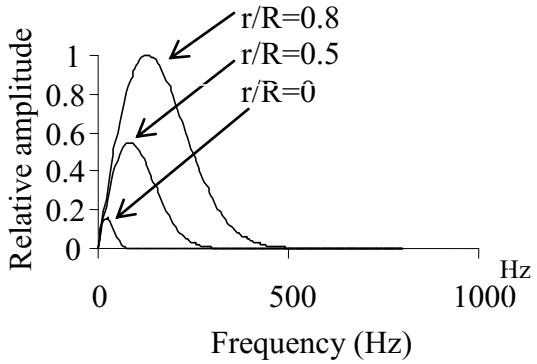

Fig.6 Predicted Frequency spatial sensitivity of the meter

where $Q^P_{NETr}(\varpi)$ is the frequency transfer function of the net charge of the roping stream of particles at radial position r , and $q^P_{NETr}(\varpi)$ is the fluctuation in the net charge. The "flow noise" is usually regarded as a band-limited white noise, as is the fluctuation in net charge $q^P_{NETr}(\varpi)$. Figure 6 shows the predicted

power spectrum of the meter at a velocity of 25m/s based on Eq. 19, where the fluctuation in net charge is assumed to be band-limited white noise having a constant power density spectrum over the effective frequency range. Typical parameters for the circuit of Fig. 5 are the following: R_n = 1 MΩ, C_n = 1.47 nF, R_d = 0.1 MΩ, and C_d = 1μF.

Spatial sensitivity expressed in the time domain

According to Parseval's formula [15], a stochastic process is related to its power spectral density function. From Eq. 19, it thus follows that

$$U_{orms} = \sqrt{\frac{1}{2\pi}\int_0^{\omega_T} |T_r(\omega)|^2 \left|q^P_{netr}(\omega)\right|^2 d\varpi} \qquad (20)$$

where $U_{o\mathrm{rms}}$ is the *rms* PF meter output, and ω_T is the effective upper cut-off frequency. If $\left|q^P_{NETr}(\varpi)\right|^2$ is white noise of value A_0 up to frequency ω_T, then the spatial sensitivity of the ring-shaped, pulverised fuel meter can be calculated using the following equation:

$$\frac{U_{rms}}{\sqrt{A_0}} = \sqrt{\frac{1}{2\pi}\int_0^{\omega_T} |T_r(\omega)|^2 d\varpi} \qquad (21)$$

Figure 7 shows the spatial sensitivity in the time domain calculated from Eq. 21.

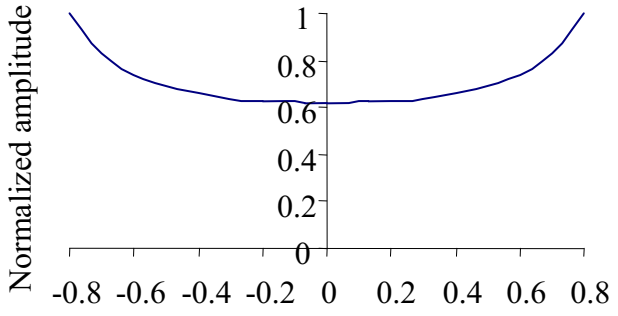

Fig. 7 Meter's Spatial Sensitivity in the Time Domain

Experimental validation

The experiments described in this section were carried out at the laboratories of Casella CRE Energy, Stoke Orchard, Cheltenham in the United Kingdom. A 14-inch (355.6-cm) diameter electrostatic meter was installed in a test facility, as depicted in Fig. 8. The

roping air-solids flowing in parallel with the pipeline were provided using a one inch (2.54-cm) diameter jet connected to the solids dispenser. A Venturi tube was located beneath the dispenser, where compressed air and solids were mixed and conveyed to the test section. The jet position in the conveyor could be adjusted both horizontally and vertically, so that the roping flow could be injected at different radii.

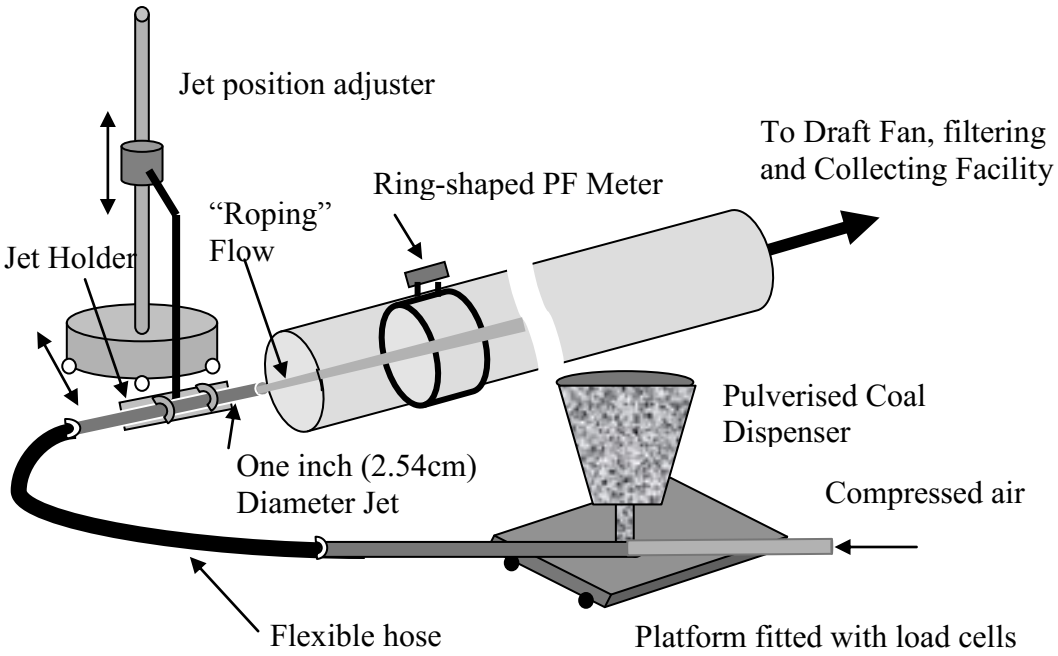

Fig.8 Spatial Sensitivity Test Facility

The flow rates of the solids and conveying air mass were monitored by computer and logged into files. Their values and their fast Fourier transforms (FFT) were calculated using National Instrument's Labview software. The sampling rate of data collection was 10kHz, and 2048 data points were collected for each measured parameter. The solids "roping" flow rate was about 300 kg/hr, and the conveying air-mass flow rate in the jet was about 60 kg/hr. The velocity of the "roping" flow was kept at about 25 m/s with the help of a draft fan at the end of the rig. Both theoretical analysis and experimental results were normalised by setting their respective maximum values to unity. The experimental results can therefore be compared to those predicted from Eqs. 19 and 21, because the net charge carried by the particles and its fluctuation level are assumed to be proportional to the solids concentration.

For the purpose of comparison, Fig. 6 is redrawn beside Fig. 9 which is based on

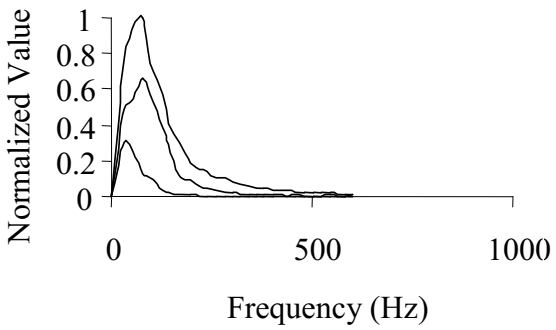

Fig.9 Test Results of frequency Response

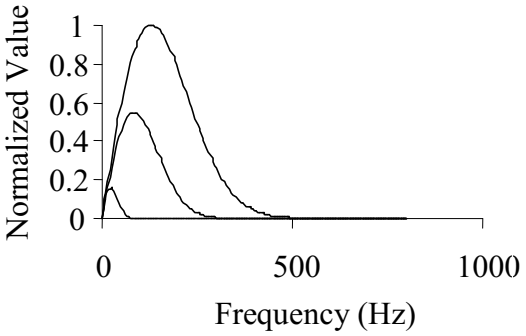

Fig.6 Predicted Frequency spatial Sensitivity of the Meter

experimental results. The shapes of the corresponding curves are similar in these two figures, except that the peak positions and the geometrical means of the curves in Fig. 9 are both shifted downward in frequency. This may have been caused by the jet vibration which would have contributed low frequency components to the flow stream. The solids moving adjacent to the pipe-wall contribute higher frequency components and have higher-level overall response, because the sensing length of the electrode along the pipeline decreases with increased relative radial position (r/R) [13].

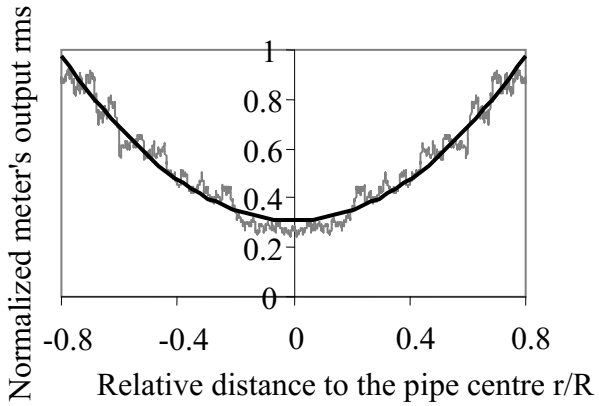

Fig. 10 Spatial sensitivity test results

The overall shape of the measured spatial response shown in Fig. 10 is similar to the calculated response shown Fig. 7. In practice, it is difficult to obtain reliable experimental spatial response results near the pipe wall where the roping flow diverges. In practice, it was very difficult to keep the roping flow perfectly constant, because the flow rate of the conveying air, as well as the pressure at the Venturi tube, changed randomly. Thus, although the curve in Fig. 10 is comprised of about 2000 data points, it is not smooth.

Verification of the assumptions used in the theoretical analysis

We assume in our theoretical analysis that the fluctuation in the charge carried by the solids is band-limited white noise. This assumption was verified by comparing the measured power spectrum of the meter with the theoretically predicted response. The measured power spectrum shown in Fig.12, caused by flow noise from pulverised fuel, compares well with the theoretical response shown in Fig. 11, although the actual

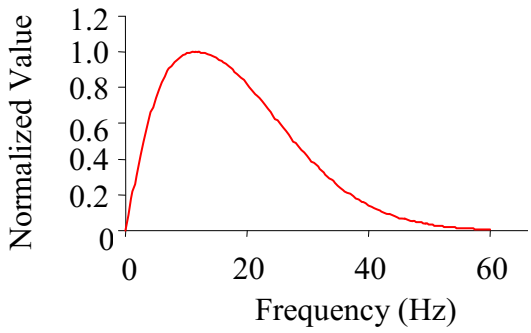

Fig. 11 Meter's Power Spectral Characteristics Based on Theoretic Analysis

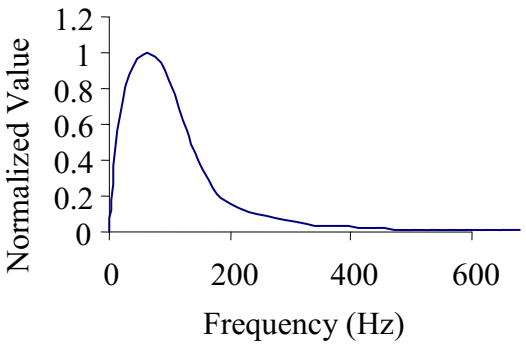

Fig. 12 Meter's Power Spectral Response Test Results

spectrum bandwidth is narrower. However, the similarity between the two figures is apparent, generally confirming the above assumptions.

Conclusions

A comparison of Figs. 6, 7, and 11 with Figs. 9, 10 and 12 confirms that the mathematical model for the response of the pulverized fuel meter is consistent with the experimental results, although a more rigorous investigation is needed. Lower frequency components dominate the meter output even though wide-band amplifiers were used. The solids

moving near the pipe wall contribute higher frequency components and have higher amplitudes than do the solids flowing near the center of the pipe.

References

[1] Huber N., Sommerfield M., "Characterization of the Cross-Sectional Particle Concentration in Pneumatic Conveying System", Powder Technology, Vol.79,1994 pp191-210

[2] Bernard J. Barry et al, "Concentration Variations within Pipe Cross-Sections in a Dilute Phase Pneumatic Conveying System", IPENZ Transactions, Vol. 24, No 1/EMCh, 1997, pp1-11

[3] Yilmaz Ali et al, "Roping Phenomena in pulverized Coal Conveying Lines", Powder Technology, Vol.93, 1998, pp 43-48

[4] Frank Thomas, et al, "Aspects of efficient parallelization of disperse gas-particle flow prediction using Eulerian-Lagrangian Approach", Proceedings of ICMF-2001, 4th International Conference on Multiphase Flow, May 21-June 1, 2001 New Orleans LA, USA Paper 311

[5] Hammer E. A., Green R. G., "'The spatial filtering effect of a capacitance transducer electrode", J. Phys.E: Sci.Instru., Vol.16, 1983, pp438-443.

[6] S. Laux, J Grusha, T. Rosin, J.D. Kersch, "ECT: More than just coal-flow monitoring", Modern power systems, March 2002, pp 22-29.

[7] Wang Shimin, et al, " Advanced Measurement and Diagnosis Technology Applied in Coal-Fired Utility Boilers", Proceedings of 5th International Symposium on Coal Combustion, Nanjing, China, November 23-26, 2003, paper No. 14

[8] DTI Project Summary 330(www.dti.gov.uk/cct/): "Pulverised Fuel Measurement with Split Control", Clean Coal Technology Programme, July 2002

[9] ECSC 7220-PR 050 Final Report, "Measurement & Control Techniques for Improving Combustion Efficiency and Reducing Emissions from Coal Fired Plant", April 2002.

[10] ECSC Coal Technical Research Programme, "On-Line Measurement of Particle Size in Fine Coal Transport system", Contract Number: 7220-PR-105, Project Commenced, Nov 2000.

[11] Zhang J., Coulthard J., Armstrong B., "Lean Phase Solids Control Using Pinch Valves and Mass Flowmeters for Pulverised Fuel", Bulk Solids Handling, Trans Tech

Publications ISSN 0173-9980 1/2003, pp34-36.

[12] Gajewski J. B., "Mathematical model of non-contact measurements of charges while moving", Journal of Electrostatics, Vol. 15, 1984, pp81-92.

[13] Cheng R., "A study of electrostatic pulverised fuel meters", Ph.D. thesis, University of Teesside, U.K. 1996.

[14] Dattaray Jagdish Rao, GE Energy, http://dattaraj_rao.tripod.com/FEM/Tutorial.html

[15] Carlson A. Bruce, "Communication Systems", An Introduction to Signal and Noise in Electrical Communication, Second Edition, McGraw Hill inc. 1975, USA pp32

Nomenclature

Symbol	**Definition**	**Symbol**	**Definition**
A	Systematic constant of a ring-shaped electrode	r_1, r_2	resistances
A_0	amplitude of band-limited white noise	r	radius of a single particle, or solids-air mixture stream line or ring shaped stream line to the pipe central line
C_d	isolating (differential) capacitance	$R_{xy}(\tau)$	cross correlation function
C_n	equivalent capacitance of a ring-shaped electrode to the earthed pipe	S	entire electrode inner surface
D	electrical flux density		
D_p	diameter of a spherical particle	$T_r(\varpi)$	transfer function of the electrostatic ring-shaped meter when a roping flow is a radius r
E	electrical field strength	U_o, $U_o(\varpi)$	output of pulverised fuel meter and its transfer function

$H_r(\varpi)$	spatial frequency response of a ring-shaped electrode to a net unit impulse charge carried by solids particles	U_{orms}	root mean square value of pulverised fuel meter output
k	systematic constant of a ring-shaped electrode	V	solids velocity
L	spacing between upstream and down stream electrodes for velocity measurement	x	co-ordinate along the pipeline
L_x	electrode sensing length along pipeline (co-ordinate x)	x(t)	signal derived on the meter installed at up stream for the solids velocity measurement
N	particle number in unit volume of air-solids mixture at position	y(t)	signal derived on the meter installed at down stream for the solids velocity measurement
N(t)	particle number time variable in unit volume of air-solids mixture	Φ	electrical potential
$P(\varpi)$	transfer function of ac-coupled pre-amplifier	Γ_i	boundary of the insulator
p	source charge		
Q, $Q(\varpi)$	charge induced on the ring-shaped electrode and its transfer function	Γ_p	boundary of the pipe
Q_{mic}	induced charges on the ring-shaped electrode due to a micro volume of air-solids mixture dr*dx at position (r,x)	Γ_t	boundary of the ring-shaped electrode

Q_{NET}^{r}	induced charge on the electrode due to net charges in a ring-shaped solids stream appeared at radius r to the pipe central line	σ_p	solids particle surface charge density
$Q_{NETr}^{P}, Q_{NETr}^{P}(\varpi)$	solids net charge roping stream at radius r to the pipe central line and its transfer function	$\delta(t)$	unit impulse function
$q_{NETr}^{P}, q_{NETr}^{P}(\varpi)$	fluctuation in the net charge carried by solids particles and its transfer function	$\delta(t-x/V)$	unit impulse waveform traveling at velocity V along the pipeline
R	inner radius of the pipe and ring-shaped electrode	ε	relative permittivity of the medium
r_d	difference resistance		
r_n	equivalent resistance of the electrode to the earthed pipe	τ	time delay
ϖ_T	effective upper cut-off frequency	τ_m	solids transient time from upstream measuring point to the down stream measuring point
∇	gradient operator	ϖ	Angular frequency